

Robust Low-rank Matrix Completion via an Alternating Manifold Proximal Gradient Continuation Method

Minhui Huang, Shiqian Ma, and Lifeng Lai

Abstract—Robust low-rank matrix completion (RMC), or robust principal component analysis with partially observed data, has been studied extensively for computer vision, signal processing and machine learning applications. This problem aims to decompose a partially observed matrix into the superposition of a low-rank matrix and a sparse matrix, where the sparse matrix captures the grossly corrupted entries of the matrix. A widely used approach to tackle RMC is to consider a convex formulation, which minimizes the nuclear norm of the low-rank matrix (to promote low-rankness) and the ℓ_1 norm of the sparse matrix (to promote sparsity). In this paper, motivated by some recent works on low-rank matrix completion and Riemannian optimization, we formulate this problem as a nonsmooth Riemannian optimization problem over Grassmann manifold. This new formulation is scalable because the low-rank matrix is factorized to the multiplication of two much smaller matrices. We then propose an alternating manifold proximal gradient continuation (AManPGC) method to solve the proposed new formulation. Convergence rate of the proposed algorithm is rigorously analyzed. Numerical results on both synthetic data and real data on background extraction from surveillance videos are reported to demonstrate the advantages of the proposed new formulation and algorithm over several popular existing approaches.

Index Terms—Robust Matrix Completion, Nonsmooth Optimization, Manifold Optimization

I. INTRODUCTION

ROBUST matrix completion (RMC) targets at fulfilling the missing entries of a partially observed matrix with the presence of sparse noisy entries. The recovery relies on a critical low-rank assumption of real datasets: a low dimensional subspace can capture most information of high-dimensional observations. Therefore, the RMC model frequently arises in a wide range of applications including recommendation systems [1], face recognition [2], collaborative filtering [3], and MRI image processing [4].

Due to its low-rank property, matrix completion can be naturally formulated as a rank constrained optimization problem. However, it is computationally intractable to directly minimize the rank function since the low-rank constraint is discrete and

nonconvex. To resolve this issue, there is a line of research focusing on convex relaxation of RMC formulations [5], [6]. For example, a widely used technique in these works is employing its tightest convex proxy, i.e. the nuclear norm. However, calculating the nuclear norm in each iteration can bring numerical difficulty for large-scale problems in practice, because algorithms for solving them need to compute a singular value decomposition (SVD) in each iteration, which can be very time consuming. Recently, nonconvex RMC formulations based on low-rank matrix factorization were proposed in the literature [7], [8], [9], [10]. In these formulations, the target matrix is factorized as the product of two much smaller matrices so that the low-rank property is automatically satisfied. The idea of factorization greatly reduces the price of promoting low-rankness, thus relieves the pressure of computation. On the other hand, researchers have also proposed the RMC problem over a fixed rank manifold [5] and solve it by manifold optimization. The retraction operation of a fixed rank manifold only requires performing a truncated SVD, thus is much more computationally efficient.

In many practical scenarios, the collected matrix datasets always come with noise. Without an effective approach to deal with these noise, recovering the ground truth of a low-rank matrix can be prevented from a reasonable solution. Fortunately, the noises in many real datasets have some common structures such as the sparsity. Therefore, it is reasonable to assume the noisy entries are sparse in matrix completion problems. To deal with the sparse noisy entries in matrix completion, researchers have employed the ℓ_1 -norm instead of the ℓ_0 -norm for decomposing sparse noisy entries in matrix completion formulations. This leads to the robust matrix completion model, which is robust to sparse outliers. In practice, the ℓ_1 -norm minimization can be efficiently solved by iterative soft thresholding in many cases. Some other robust loss functions such as the Huber loss were also proposed in the literature [11].

In this paper, by utilizing the recent developments on manifold optimization, we propose a nonsmooth RMC formulation over the Grassmann manifold with a properly designed regularizer. The Grassmann manifold automatically restricts our factorizer on a fixed dimension subspace, thus promotes the fixed low rank property. In each iteration, we only require a QR decomposition as our retraction for the Grassmann manifold, which is more computationally efficient compared with the truncated SVD. Notice that in [12], the author designed a regularizer to balance the scale of two factorizers. In our

M. Huang and L. Lai are with the Department of Electrical and Computer Engineering, University of California, Davis, CA, 95616. Email: {mhhuang, llfai}@ucdavis.edu.

S. Ma is with the Department of Mathematics, University of California, Davis, CA, 95616. Email: sqma@ucdavis.edu.

This research was partially supported by NSF HDR TRIPODS grant CCF-1934568, NSF grants CCF-1717943, CNS-1824553, CCF-1908258, DMS-1953210 and CCF-2007797, and UC Davis CeDAR (Center for Data Science and Artificial Intelligence Research) Innovative Data Science Seed Funding Program.

formulation, the QR decomposition automatically balances the scale of two factorizers, which prevents our formulation from being ill-conditioned. Moreover, compared with previous work on matrix completion over Grassmann manifold [13], [14], [15], [16], our formulation is continuous with a smaller searching space. We then propose an alternating manifold proximal gradient (AManPG) algorithm for solving it. The AManPG algorithm alternately updates between the low-rank factorizer with a Riemannian gradient step and the nonsmooth sparse variable with a proximal gradient step. While recent ADMM based methods [10], [17], [18] lack any convergence guarantee, we can rigorously analyze the convergence of AManPG algorithm and prove a complexity bound of $\mathcal{O}(\epsilon^{-2})$ to reach an ϵ -stationary point. Furthermore, compared with recent smoothing technique developed in [5], we solve the nonsmooth subproblem directly. To further boost the convergence speed and recover the low-rank matrix with a high accuracy, we apply a continuation framework [19] to AManPG. Finally, we conduct extensive numerical experiments and show that the proposed AManPG with continuation is more efficient compared with previous works on the RMC problem.

The remainder of the paper is organized as follows. In Section II, we briefly review some existing related work on the RMC problem and give our new RMC formulation over Grassmann manifold. In Section III, we review some basics of manifold optimization and propose ManPG algorithm for our RMC formulation. In Section IV and Section V, we propose our AManPG with continuation algorithm and provide its convergence analysis. In Section VI, numerical results are presented to demonstrate the advantages of the proposed new formulation and algorithm. Finally, the conclusions are given in Section VII.

II. PROBLEM FORMULATION

In this section, to motivate our proposed problem formulation, we will first introduce some closely related work. We then present our problem formulation.

A. Related Work

Robust principal component analysis (PCA) [20], [21] is an important tool in data analysis and has found many interesting applications in computer vision, signal processing, machine learning, and statistics, and so on. The goal is to decompose a given matrix $M \in \mathbb{R}^{m \times n}$ into the superposition of a low-rank matrix L and a sparse matrix S , i.e., $M = L + S$. The works by Candès et al. [20] and Chandrasekaran et al. [21] formulate the problem as the following convex optimization problem:

$$\min_{L, S} \|L\|_* + \gamma \|S\|_1, \text{ s.t. } L + S = M, \quad (1)$$

where $\gamma > 0$ is a weighting parameter, the nuclear norm $\|L\|_*$ sums the singular values of L , and the ℓ_1 norm $\|S\|_1$ sums the absolute values of all entries of S . When only a subset of the entries of M is observed, robust PCA becomes the robust low-rank matrix completion problem [5]. Similar to (1), a convex formulation for RMC can be cast as follows:

$$\min_{L, S} \|L\|_* + \gamma \|S\|_1, \text{ s.t. } \mathcal{P}_\Omega(L + S) = \mathcal{P}_\Omega(M), \quad (2)$$

where Ω denotes the set of the indices of the observed entries and $\mathcal{P}_\Omega : \mathbb{R}^{m \times n} \mapsto \mathbb{R}^{m \times n}$ denotes a projection defined as: $[\mathcal{P}_\Omega(Z)]_{ij} = Z_{ij}$, if $(i, j) \in \Omega$, and $[\mathcal{P}_\Omega(Z)]_{ij} = 0$, otherwise. The convex formulations (1) and (2) have been studied extensively in the literature, and we refer to the recent survey paper [6] for algorithms for solving them.

By assuming that the rank of L is known (denoted by r), the idea of many nonconvex formulations is based on the fact that L can be factorized to $L = UV$, where $U \in \mathbb{R}^{m \times r}$, $V \in \mathbb{R}^{r \times n}$. Replacing L by UV in (1) and (2) leads to various nonconvex formulations for robust PCA and RMC. In particular, Li et al. [12] suggested using subgradient method to solve the following nonsmooth robust matrix recovery model

$$\min_{U \in \mathbb{R}^{m \times r}, V \in \mathbb{R}^{r \times n}} \frac{1}{|\Omega|} \|y - \mathcal{A}(UV)\|_1, \quad (3)$$

where y is a small number of linear measurements and $\mathcal{A} : \mathbb{R}^{m \times n} \rightarrow \mathbb{R}^{|\Omega|}$ is a known linear operator. Shen et al. [10] proposed the LMaFit algorithm that implements an alternating direction method of multipliers (ADMM) for solving the following nonconvex formulation of robust PCA:

$$\begin{aligned} \min_{U \in \mathbb{R}^{m \times r}, V \in \mathbb{R}^{r \times n}, Z \in \mathbb{R}^{m \times n}} \quad & \|\mathcal{P}_\Omega(Z - M)\|_1, \\ \text{s.t.} \quad & UV - Z = 0. \end{aligned} \quad (4)$$

Note that if (\hat{U}, \hat{V}) solves (4), then $(\hat{U}Q, Q^{-1}\hat{V})$ also solves (4) for any invertible $Q \in \mathbb{R}^{r \times r}$. Since all matrices $\hat{U}Q$ share the same column space, Dai et al. [13], [14] exploited this fact and formulated the matrix completion problem as the following optimization problem over a Grassmann manifold:

$$\min_{U \in \text{Gr}(m, r), V \in \mathbb{R}^{r \times n}} \|\mathcal{P}_\Omega(UV - M)\|_F^2, \quad (5)$$

where $\text{Gr}(m, r)$ denotes the Grassmann manifold. However, it is noticed that the outer problem for U might be discontinuous at points U for which the V problem does not have a unique solution. To address this issue, Keshavan et al. [15], [16] proposed to optimize both the column space and row space at the same time, which results in the following so-called OptSpace formulation for matrix completion:

$$\begin{aligned} \min_{U \in \text{Gr}(m, r), V \in \text{Gr}(n, r), \Sigma \in \mathbb{R}^{r \times r}} \quad & \|\mathcal{P}_\Omega(U\Sigma V^\top - M)\|_F^2 \\ & + \lambda \|U\Sigma V^\top\|_F^2. \end{aligned} \quad (6)$$

Here $\lambda > 0$ is a weighting parameter, and the regularizer $\|U\Sigma V^\top\|_F^2$ is used so that the outer problem is continuous. Boumal and Absil [22], [23] proposed to study the following variant of (5):

$$\min_{U \in \text{Gr}(m, r), V \in \mathbb{R}^{r \times n}} \frac{1}{2} \|\mathcal{P}_\Omega(UV - M)\|_F^2 + \frac{\lambda^2}{2} \|\mathcal{P}_{\bar{\Omega}}(UV)\|_F^2, \quad (7)$$

where $\bar{\Omega}$ is the complement of Ω , and they proposed to use Riemannian trust region method to solve this problem. Comparing with OptSpace (6), formulation (7) has a much smaller searching space. Note that in (7), λ is usually chosen to be very close to zero, as it indicates that we have a small confidence that the entries $(UV)_{ij}$ for $(i, j) \notin \Omega$ are equal to zero.

For RMC, Cambier and Absil [5] proposed the following Riemannian optimization formulation:

$$\min_{X \in \mathcal{M}_r} \|\mathcal{P}_\Omega(X - M)\|_1 + \lambda \|\mathcal{P}_\Omega(X)\|_F^2, \quad (8)$$

where \mathcal{M}_r denotes the fixed-rank manifold, i.e., $\mathcal{M}_r := \{X \mid \text{rank}(X) = r\}$. The algorithm proposed in [5] needs to smooth the ℓ_1 norm first to change the problem to a smooth problem, and then applies the Riemannian conjugate gradient method to solve the smoothed problem. As a result, the algorithm in [5] does not solve (8) exactly. Related to (5) and (4), He et al. proposed the GRASTA algorithm [17], [18] which can be used to solve the following formulation of RMC:

$$\min_{U \in \text{Gr}(m,r), V \in \mathbb{R}^{r \times n}} \|\mathcal{P}_\Omega(UV - M)\|_1. \quad (9)$$

GRASTA uses alternating minimization and ADMM to solve (9), which is efficient in practice but lacks convergence guarantees. Moreover, Zhao et al. [11] explores the effect of different robust loss functions for proposing the robustness against specific categories of outliers. He et al. [24] derived a correntropy-based cost function and applied the half-quadratic technique to solve the formulation. Zeng et al. [25] proposed two schemes, namely the iterative ℓ_p -regression algorithm and ADMM for RMC under ℓ_p minimization. Zhang et al. [26] proposed the RMC problem over Hankel matrix and claimed that they can deal with case when all the observations in one column are erroneous.

B. Our formulation and contributions

Motivated by these existing works, in this paper, we propose to solve the following formulation of RMC:

$$\min_{U \in \text{Gr}(m,r), V \in \mathbb{R}^{r \times n}, S \in \mathbb{R}^{m \times n}} F(U, V, S) = \frac{1}{2} \|\mathcal{P}_\Omega(UV - M + S)\|_F^2 + \frac{\lambda^2}{2} \|\mathcal{P}_\Omega(UV)\|_F^2 + \gamma \|\mathcal{P}_\Omega(S)\|_1. \quad (10)$$

We show that the manifold proximal gradient method (ManPG) proposed by Chen et al. [27] can be applied to solve (10) and the corresponding convergence analysis applies naturally. We then propose a variant of ManPG, named alternating ManPG (AManPG) that can significantly improve the efficiency of ManPG for solving (10). We further rigorously analyze the convergence rate of AManPG. Compared with GRASTA, our proposed algorithms for solving (10) have rigorous convergence guarantees and convergence rate analysis. Compared with RMC (8), our algorithms solve the nonsmooth problem (10) directly. Compared with the convex formulation (2), our nonconvex formulation appears to be more robust and scalable, see the numerical experiments for comparison results. Finally, to further accelerate the convergence of AManPG, we incorporate the so-called continuation technique on the weighting parameter γ in (10). Our numerical results on both synthetic data and real data on background extraction from surveillance video demonstrate that our final algorithm, AManPG with Continuation (AManPGC), compares favorably with existing methods for RMC.

III. THE MANPG ALGORITHM FOR ROBUST MATRIX COMPLETION

In this section, we show that the ManPG algorithm recently proposed by Chen et al. [27] can be naturally adopted to solve (10). Note that the ManPG algorithm was originally proposed for solving problems over the Stiefel manifold, but the manifold in (10) is Grassmann manifold. Therefore, we need to further elaborate on the details how ManPG works on Grassmann manifold. To this end, we first introduce some backgrounds on the geometry of Grassmann manifold.

A. Geometry of the Grassmann Manifold

In this subsection we briefly introduce concepts and properties of Grassmann manifold. Much of the materials here are from [22], and we include them here for the ease of discussion later. Grassmann manifold $\text{Gr}(m, r)$ is the set of r -dimensional linear subspaces of \mathbb{R}^m endowed with quotient manifold structure, whose dimension is $\dim(\text{Gr}(m, r)) = r(m - r)$ [28]. Each point of $\text{Gr}(m, r)$ is a linear subspace spanned by the column space of a full-rank matrix U :

$$\text{Gr}(m, r) = \{\text{span}(U) : U \in \mathbb{R}_*^{m \times r}\}, \quad (11)$$

where $\mathbb{R}_*^{m \times r}$ denotes the set of all $m \times r$ matrices with full column rank, and $\text{span}(U)$ denotes the subspace spanned by the columns of U . Since multiplying by an $r \times r$ orthonormal matrix does not change the column space of U , we can regard $\text{Gr}(m, r)$ as a quotient of $\mathbb{R}_*^{m \times r}$ by the equivalent relation $U' = UQ$, where Q is any $r \times r$ orthonormal matrices. Endowed with the Riemannian metric $\langle U, V \rangle = \text{Tr}(UV)$, the Grassmann manifold is also a Riemannian quotient manifold, and it admits a tangent space at each point of $\text{Gr}(m, r)$ given by

$$\text{T}_U \text{Gr}(m, r) = \{H \in \mathbb{R}^{m \times r} : U^\top H = 0\}. \quad (12)$$

For Riemannian manifold \mathcal{M} , the Riemannian gradient of a smooth function $f : \mathcal{M} \rightarrow \mathbb{R}$ is defined as follows.

Definition III.1. (Riemannian Gradient) Given a smooth function $f : \mathcal{M} \rightarrow \mathbb{R}$, the Riemannian gradient of f at $X \in \mathcal{M}$, denoted by $\text{grad}f(X)$, is the unique tangent vector in $\text{T}_X \mathcal{M}$ such that

$$\langle \text{grad}f(X), \xi \rangle = Df(X)[\xi], \quad \forall \xi \in \text{T}_X \mathcal{M}, \quad (13)$$

where Df denotes the directional derivatives of f .

For Grassmann manifold, the orthogonal projector from $\mathbb{R}^{m \times r}$ onto the tangent space $\text{T}_U \text{Gr}(m, r)$ is given by:

$$\begin{aligned} \text{Proj}_U : \mathbb{R}^{m \times r} &\rightarrow \text{T}_U \text{Gr}(m, r), \\ \text{Proj}_U(H) &= (I - UU^\top)H. \end{aligned} \quad (14)$$

The definition of retraction operation for manifold \mathcal{M} is given below.

Definition III.2. (Retraction) Let $\text{Retr}_X(\xi) : \text{T}\mathcal{M} \rightarrow \mathcal{M}$ be a mapping from the tangent bundle $\text{T}\mathcal{M}$ to the manifold \mathcal{M} . We call $\text{Retr}_X(\cdot)$ a retraction at X if

$$\begin{aligned} \text{Retr}_X(0) &= X, \quad \frac{d}{dt} \text{Retr}_X(t\xi)|_{t=0} = \xi, \\ \forall X \in \mathcal{M}, \quad \forall \xi \in \text{T}_X \mathcal{M}. \end{aligned} \quad (15)$$

In our numerical experiments, we choose the QR decomposition as the retraction for Grassmann manifold:

$$\text{Retr}_U(H) = \text{qf}(U + H), \quad (16)$$

where $\text{qf}(X)$ denotes the Q -factor of the QR decomposition of X .

B. The ManPG Algorithm

Recently, Chen et al. [27] proposed a novel ManPG algorithm for solving nonsmooth optimization problem over the Stiefel manifold $\text{St}(n, r)$ in the following form:

$$\min_{X \in \text{St}(n, r)} F_1(X) + F_2(X), \quad (17)$$

in which F_1 is smooth with Lipschitz continuous gradient, F_2 is nonsmooth and convex. Here the smoothness, convexity and Lipschitz continuity are interpreted when the functions are considered in the ambient Euclidean space. A typical iteration of ManPG algorithm for solving (17) is as follows:

$$\begin{aligned} Y^k &:= \underset{Y}{\text{argmin}} \langle \nabla F_1(X^k), Y \rangle + \frac{1}{2t} \|Y\|_F^2 \\ &\quad + F_2(X^k + Y), \text{ s.t.}, Y \in \mathbb{T}_{X^k} \text{St}(n, r) \\ X^{k+1} &:= \text{Retr}_{X^k}(\alpha_k Y^k), \end{aligned} \quad (18)$$

where $t > 0$ and $\alpha_k > 0$ are step sizes. Chen et al. [27] proved that the iteration complexity of ManPG (18) is $O(1/\epsilon^2)$ for obtaining an ϵ -stationary solution. They also demonstrated that ManPG is very efficient for solving sparse PCA and compressed modes problems.

Now we discuss how to apply ManPG [27] to solve (10). For ease of presentation, we denote the smooth part of F in (10) by \bar{f} , i.e.,

$$\bar{f}(U, V, S) = \frac{1}{2} \|\mathcal{P}_\Omega(UV - M + S)\|_F^2 + \frac{\lambda^2}{2} \|\mathcal{P}_\Omega(UV)\|_F^2. \quad (19)$$

Note that for fixed U and S , the optimal V of $F(U, V, S)$ (and $\bar{f}(U, V, S)$) is uniquely determined. Therefore, by denoting

$$V_{U,S} := \underset{V}{\text{argmin}} \bar{f}(U, V, S), \quad (20)$$

and

$$f(U, S) = \bar{f}(U, V_{U,S}, S), \quad (21)$$

we know that our RMC formulation (10) reduces to

$$\min_{U \in \text{Gr}(m, r), S \in \mathbb{R}^{m \times n}} f(U, S) + \gamma \|\mathcal{P}_\Omega(S)\|_1. \quad (22)$$

It is easy to see that ManPG for solving (22) reduces to the following two subproblems in the k -th iteration:

$$\begin{aligned} \Delta S^k &:= \underset{\Delta S}{\text{argmin}} \langle \nabla_S f(U^k, S^k), \Delta S \rangle + \frac{1}{2t_S} \|\Delta S\|_F^2 \\ &\quad + \gamma \|\mathcal{P}_\Omega(S^k + \Delta S)\|_1 \end{aligned} \quad (23a)$$

$$\begin{aligned} \Delta U^k &:= \underset{\Delta U}{\text{argmin}} \langle \nabla_U f(U^k, S^k), \Delta U \rangle + \frac{1}{2t_U} \|\Delta U\|_F^2, \\ \text{s.t.}, \Delta U &\in \mathbb{T}_{U^k} \text{Gr}(m, r) \end{aligned} \quad (23b)$$

$$S^{k+1} := S^k + \alpha \Delta S^k, \quad (23c)$$

$$U^{k+1} := \text{Retr}_{U^k}(U^k + \beta \Delta U^k), \quad (23d)$$

Algorithm 1 ManPG for solving RMC (22)

- 1: Input: step sizes t_S, t_U, α, β , parameters λ, γ , accuracy tolerance ϵ , and initial point (U^0, S^0) .
 - 2: **for** $k = 0, 1, \dots$ **do**
 - 3: Compute V_{U^k, S^k}^k using (27)
 - 4: Compute ΔS^k by (25)
 - 5: Update S^{k+1} by (23c)
 - 6: Compute ΔU^k by (24)
 - 7: Update U^{k+1} by (23d)
 - 8: **if** $\|\Delta U^{k+1}\|_F^2 + \|\Delta S^{k+1}\|_F^2 \leq \epsilon^2$ **then**
 - 9: **break**
 - 10: **end if**
 - 11: **end for**
 - 12: Output: U^{k+1}, S^{k+1}
-

where t_S, t_U, α and β are all step sizes. We now make some necessary remarks on this ManPG algorithm (23). First, (23) is actually slightly different with a direct application of ManPG for solving (22). For a direct application of ManPG, we should have $t_S = t_U$ and $\alpha = \beta$. Here in (23) we allow these step sizes to be different so that we have more freedom to choose the best step sizes in practice. Also we note that (23b) and (23d) correspond to a Riemannian gradient step with respect to the U variable. The updates (23a) and (23c) correspond to a proximal gradient step for the S variable in the Euclidean space. This can be interpreted in the following way. First, in RMC (22), the U variable does not appear in the nonsmooth part of the objective, so it is natural to perform a Riemannian gradient step for U . Second, for fixed U , the S problem is only an unconstrained problem in the Euclidean space, so it is reasonable to take a proximal gradient step. Moreover, the two subproblems (23b) and (23a) are very easy to solve.

Specifically, (23b) can be reduced to

$$\Delta U^k = -t_U \text{grad}_U f(U^k, S^k), \quad (24)$$

i.e., it is the negative Riemannian gradient of f multiplied by the step size t_U . The ΔS subproblem (23a) can be solved by a simple ℓ_1 norm shrinkage operation (note that we are only interested in the $\mathcal{P}_\Omega(\Delta S^k)$ and $\mathcal{P}_\Omega(\Delta S^k)$ can be simply set to 0):

$$\begin{aligned} \mathcal{P}_\Omega(\Delta S^k) &= \text{Prox}_{\gamma t_S \|\cdot\|_1}(\mathcal{P}_\Omega(S^k - t_S \nabla_S f(U^k, S^k))) \\ &\quad - \mathcal{P}_\Omega(S^k). \end{aligned} \quad (25)$$

Now, to implement the ManPG (23), the only remaining component is to calculate the Riemannian gradient $\text{grad}_U f(U, S)$ used in (24). The procedure for computing it is outlined in [23]. By assuming that the subspace of the Grassmann manifold is represented by orthonormal bases, which means U is restricted to the Stiefel manifold, the Riemannian gradient of the smooth function $f(U, S)$ with respect to U is given by:

$$\begin{aligned} \text{grad}_U f(U, S) &= ((1 - \lambda^2)C \odot (UV_{U,S} - M + S) - \\ &\quad \lambda^2(M - S))V_{U,S}^\top + \lambda^2 U(V_{U,S}V_{U,S}^\top), \end{aligned} \quad (26)$$

where $C \in \mathbb{R}^{m \times n}$ is the mask operator whose components are given by: $C_{ij} = 1$ if $(i, j) \in \Omega$, and $C_{ij} = 0$ otherwise. Here $V_{U,S}$ is defined in (20), and it can be computed as follows:

$$\text{vec}(V_{U,S}) = A^{-1} \text{vec}(U^\top [C \odot (M - S)]), \quad (27)$$

where vec denotes the vectorization operator, and A is defined as

$$A = (I_n \otimes U^\top) \text{diag}(\text{vec}((1 - \lambda^2)C))(I_n \otimes U) + \lambda^2 I_{rn}.$$

and \otimes denotes the Kronecker product. For more details about these calculation, we refer the reader to [23].

With these preparations, we can finally summarize the ManPG algorithm (23) for solving (10) (or, (22)) as in Algorithm 1.

IV. ALTERNATING MANPG WITH CONTINUATION

It should be noted that ManPG updates S and U in parallel. That is, ManPG (23) is a Jacobi type iterative algorithm. One way that can possibly improve the speed of ManPG is to use a Gauss-Seidel type algorithm. This idea has also been adopted in [29], where the authors showed that the Gauss-Seidel type ManPG performs much better than the original Jacobi type ManPG. Motivated by this, here we also propose an alternating ManPG (AManPG), which updates S and U sequentially, instead of in parallel. However, one crucial thing to note here is that the V variable will need to be re-calculated, when we have a new S variable before we update the U variable. Our AManPG algorithm is summarized in Algorithm 2.

Algorithm 2 AManPG for solving (22)

- 1: Input: step sizes t_S, t_U, α, β , parameters λ, γ , threshold ϵ, U^0, S^0 .
 - 2: **for** $k = 0, 1, \dots$ **do**
 - 3: Compute V_{U^k, S^k}^k using (27)
 - 4: Compute ΔS^k by (25)
 - 5: Update S^{k+1} by (23c)
 - 6: Compute $V_{U^k, S^{k+1}}^k$ using (27)
 - 7: Compute $\Delta U^k = -t_U \text{grad}_U f(U^k, S^{k+1})$
 - 8: Update U^{k+1} by (23d)
 - 9: **if** $\|\Delta U^{k+1}\|_F^2 + \|\Delta S^{k+1}\|_F^2 \leq \epsilon^2$ **then**
 - 10: **break**
 - 11: **end if**
 - 12: **end for**
 - 13: Output: U^{k+1}, S^{k+1}
-

Remark IV.1. When we compute ΔU^k in AManPG, we used the latest S^{k+1} , which requires us to compute the latest $V_{U^k, S^{k+1}}^k$. While in ManPG, we used S^k in the updates of ΔU^k , and this does not require us to compute another V^k . This is the main difference between AManPG (Algorithm 2) and ManPG (Algorithm 1). In both algorithms, we always set $\alpha = \beta = 1$. Noticing that the matrix A only depends on variable U , there is no need to recalculate A when computing $V_{U^k, S^{k+1}}^k$.

Algorithm 3 AManPG with Continuation (AManPGC) for solving (22)

- 1: Input: Step sizes t_S, t_U , parameters $\gamma_0 \gg \gamma_{\min}$, shrinking factors $\mu_1 < 1, \mu_2 < 1$, initial accuracy tolerance ϵ^0
 - 2: Initialize: U^0, S^0 . Set $\ell = 0$
 - 3: **while** $\gamma_\ell > \gamma_{\min}$ **do**
 - 4: Call AManPG to solve (22) with $\gamma = \gamma_\ell$, and set the output of AManPG as $(U^{\ell+1}, S^{\ell+1})$.
 - 5: $\gamma_{\ell+1} = \mu_1 \gamma_\ell$
 - 6: $\epsilon_{\ell+1} = \mu_2 \epsilon_\ell$
 - 7: $\ell = \ell + 1$
 - 8: **end while**
 - 9: Output: U^ℓ, S^ℓ
-

The continuation technique. There are two parameters in the model (10): λ and γ . Since λ indicates our confidence level of the entries of (UV) being zero, it needs to very small. In practice, it is easy to choose λ , and in our numerical experiments, we always choose $\lambda = 10^{-8}$. The parameter γ in (10) controls the sparsity level of $\mathcal{P}_\Omega(S)$. A larger γ yields sparser $\mathcal{P}_\Omega(S)$. However, in practice, we usually have no clue how sparse the matrix S should be. Thus, it is not easy to choose γ . A usual practice in the literature to deal with this issue is to conduct a continuation technique on γ . Roughly speaking, the continuation starts with solving (10) with a relatively large γ . Then the parameter γ is decreased and (10) is solved again. This process is repeated until γ is very small. This idea has been widely adopted in the literature, e.g., [19], [30], [31], [32]. Combining this continuation idea with our AManPG algorithm, we obtain the AManPGC algorithm which works greatly in practice as confirmed by our numerical results in Section VI. AManPGC is summarized in Algorithm 3. Note that in Algorithm 3, we also shrink the accuracy tolerance ϵ in each iteration, as we want to solve the problem more and more accurately.

V. CONVERGENCE ANALYSIS FOR AMANPG

In this section, we analyze the convergence behavior and iteration complexity of AManPG (Algorithm 2). To simplify the notation, we denote $\mathcal{M} = \text{Gr}(m, r)$ and $h(S) = \gamma \|\mathcal{P}_\Omega(S)\|_1$, and we analyze the convergence of AManPG for solving the following problem:

$$\min F(U, S) = f(U, S) + h(S), \quad \text{s.t.}, \quad U \in \mathcal{M}, \quad (28)$$

where $f(U, S)$ is smooth and $h(S)$ is nonsmooth and convex. Here the smoothness and convexity are interpreted when the functions are considered in the ambient Euclidean space. For simplicity, we rewrite the AManPG for solving (28) here. One

typical iteration of AManPG for solving (28) is:

$$\begin{aligned} \Delta S^k := & \underset{\Delta S}{\operatorname{argmin}} \langle \nabla_S f(U^k, S^k), \Delta S \rangle + \frac{1}{2t_S} \|\Delta S\|_F^2 \\ & + h(S^k + \Delta S), \end{aligned} \quad (29a)$$

$$S^{k+1} := S^k + \alpha \Delta S^k, \quad (29b)$$

$$\begin{aligned} \Delta U^k := & \underset{\Delta U}{\operatorname{argmin}} \langle \nabla_U f(U^k, S^{k+1}), \Delta U \rangle + \frac{1}{2t_U} \|\Delta U\|_F^2, \\ \text{s.t. } & \Delta U \in \mathbb{T}_{U^k} \mathcal{M} \end{aligned} \quad (29c)$$

$$U^{k+1} := \operatorname{Retr}_{U^k}(U^k + \beta \Delta U^k). \quad (29d)$$

We make the following assumptions of (28) throughout this section.

Assumption V.1. (*F is lower bounded*) There exists a finite constant F^* , such that

$$F(X) \geq F^*, \quad \forall X \in \mathcal{M}.$$

Note that for (22), it is easy to see that $F^* = 0$.

Assumption V.2. (*Lipschitz Continuity of $\nabla_S f(U, S)$*) The gradient $\nabla_S f(U, S)$ is Lipschitz continuous with Lipschitz constant L_S . That is

$$\|\nabla_S f(U, S_1) - \nabla_S f(U, S_2)\|_F \leq L_S \|S_1 - S_2\|_F, \quad \forall S_1, S_2 \in \mathbb{R}^{m \times n}, U \in \mathcal{M}.$$

The following assumption is about $\operatorname{grad}_U f(U, S)$, which regards the regularity of the pullback function $\hat{f}(\Delta U, S) = f(\operatorname{Retr}_U(\Delta U), S)$, and differs from the standard Lipschitz continuity assumption because of the retraction operator. This assumption was originally suggested in [33].

Assumption V.3. (*Restricted Lipschitz-type gradient for pullbacks*) There exists $L_U \geq 0$ such that, for sequence $(U^k, S^k)_{k \geq 0}$ generated by AManPG (Algorithm 2), the pullback function $\hat{f}_k(\Delta U) = f(\operatorname{Retr}_{U^k}(\Delta U), S^{k+1})$ satisfies

$$\begin{aligned} & \left| \hat{f}_k(\Delta U) - [f(U^k, S^{k+1}) + \langle \Delta U, \operatorname{grad}_U f(U^k, S^{k+1}) \rangle] \right| \\ & \leq \frac{L_U}{2} \|\Delta U\|_F^2, \quad \forall \Delta U \in \mathbb{T}_{U^k} \mathcal{M}. \end{aligned}$$

From the Theorem 4.1 in [34], we can define the stationary point of problem (28) as follows.

Definition V.4. (*Stationary point*). A pair of $(U, S) \in \mathcal{M} \times \mathbb{R}^{m \times n}$ is called a stationary point of problem (28) if it satisfies the first-order necessary conditions:

$$0 = \operatorname{grad}_U f(U, S), \quad 0 \in \nabla_S f(U, S) + \partial h(S). \quad (30)$$

According to Theorem 4.1 in [34], the optimality conditions of the subproblems (29c) and (29a) are

$$\begin{aligned} 0 & = \operatorname{grad}_U f(U^k, S^{k+1}) + \frac{1}{t_U} \Delta U^k, \\ 0 & \in \frac{1}{t_S} \Delta S^k + \nabla_S f(U^k, S^k) + \partial h(S^k + \Delta S^k). \end{aligned} \quad (31)$$

If $\Delta U^k = 0$ and $\Delta S^k = 0$, then we know that $S^{k+1} = S^k$, and (U^k, S^k) satisfies (30) and thus is a stationary point of (28). Therefore, we can use the norm of (U^k, S^k) to measure the closeness to stationary point, and we define the ϵ -stationary point of (28) as follows.

Definition V.5. (*ϵ -stationary point*). We say that $(U^k, S^k) \in \mathcal{M} \times \mathbb{R}^{m \times n}$ is an ϵ -stationary point of (28), if $(\Delta S^k, \Delta U^k)$ given by (29a) and (29c) satisfies

$$\|\Delta S^k\|_F^2 + \|\Delta U^k\|_F^2 \leq \epsilon^2 / L^2, \quad (32)$$

where $L := \min\{L_S, L_U\}$.

Now we are ready to analyze the iteration complexity of AManPG for obtaining an ϵ -stationary point of (28). First, we prove two lemmas, which show that there is a sufficient reduction of the objective value after each update of S and U .

Lemma V.6. Assume Assumption V.2 holds, and the sequence $(S^k, U^k, \Delta S^k, \Delta U^k)$ is generated by AManPG. By choosing $t_S = 1/L_S$ and $\alpha = 1$, the following inequality holds

$$F(U^k, S^{k+1}) - F(U^k, S^k) \leq -\frac{L_S}{2} \|\Delta S^k\|_F^2. \quad (33)$$

Proof. Please see Appendix A for details. \square

Lemma V.7. Assume Assumption V.3 holds, and the sequence $(S^k, U^k, \Delta S^k, \Delta U^k)$ is generated by AManPG. By choosing $t_U = 1/L_U$ and $\beta = 1$, the following inequality holds

$$F(U^{k+1}, S^{k+1}) - F(U^k, S^{k+1}) \leq -\frac{L_U}{2} \|\Delta U^k\|_F^2. \quad (34)$$

Proof. Please see Appendix B for details. \square

Now we are ready to present our main convergence result of AManPG.

Theorem V.8. Assume Assumptions V.1, (V.2) and (V.3) hold. By choosing $t_U = 1/L_U$, $t_S = 1/L_S$, $\alpha = \beta = 1$ in AManPG (29), every limit point of the sequence $\{U^k, S^k\}$ generated by AManPG (29) is a stationary point of problem (28). Moreover, AManPG (29) returns an ϵ -stationary point of problem (28) in at most $\lceil 2L(F(U^0, S^0) - F^*)/\epsilon^2 \rceil$ iterations, where $L := \min(L_S, L_U)$.

Proof. Please see Appendix C for details. \square

VI. NUMERICAL EXPERIMENTS

In this section, we provide numerical results for both synthetic and real datasets to verify the performance of the proposed algorithms. We focus on comparing our ManPG and AManPG algorithms with some baseline algorithms using the robustness of ℓ_1 -norm, in particular, the subgradient method (SubGM) [12], the LMafit [10] and the Riemannian conjugate gradient method for the smoothed ℓ_1 -norm objective function (RMC) [5]. We use the same continuation framework for ManPG and call it ManPGC. For the SubGM method, we assume that the linear operator \mathcal{A} is a simple projection. For the LMafit algorithm, we turn off the rank estimation since we assume that the rank is known for all cases. We use the original setting for the RMC algorithm. All algorithms use same C-Mex code for accelerating the matrix multiplication between a sparse matrix and a full matrix and some other bottleneck computations. Moreover, to guarantee a fair comparison, each algorithm is carefully tuned to achieve its best performance. All experiments were run on Matlab R2018b with a 2.3 GHz Dual-Core Intel Core i5 CPU.

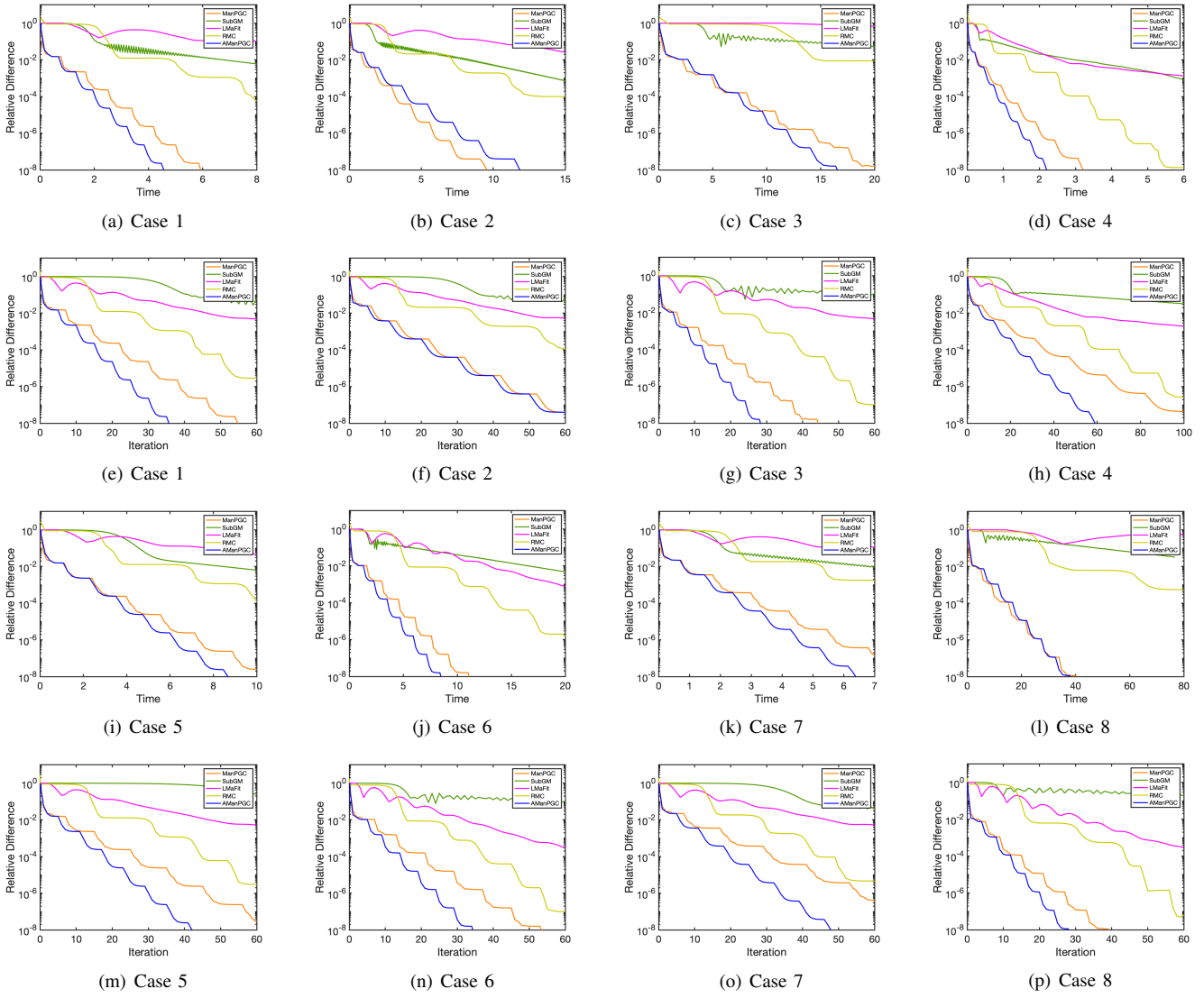


Fig. 1. Relative difference for synthetic data on different cases. (a), (b), (c), (d), (i), (j), (k), (l) present the CPU time comparison; (e), (f), (g), (h), (m), (n), (o), (p) present the running iteration comparison.

A. Synthetic Data

We first test our ManPGC and AManPGC algorithms on different cases of synthetic data. After picking the values of m, n, r , we generate the ground truth $U^* \in \mathbb{R}^{m \times r}$, $V^* \in \mathbb{R}^{r \times n}$ with i.i.d. normal entries of zero mean and unit variance. The target matrix is $X^* = U^*V^*$. We then choose a sampling ratio and sample entries uniformly at random to get the observed matrix M . Finally, we add a sparse matrix S^* , whose nonzero entries are generated by a normal distribution with zero mean and unit variance with a sparsity rate, to the observed matrix M .

Parameters: In our experiment, we observe that by setting $t_S = 1$, we get very good performance. Due to the problem formulation (10), $t_S = 1$ gives us a direct proximal mapping for the S subproblem when we fix V_{U^k, S^k} . We tune t_U between $1/|\Omega|$ and $3/|\Omega|$ and set $\gamma_0 = 10$, $\lambda = 10^{-8}$, $\mu_1 = \mu_2 = 1/10$ in all experiments. We use different ϵ_0 values specified in the following cases. We may use any random matrix U_0 as

our initial point, but in practice, we use the singular value decomposition of the observed matrix M as our initial point for all algorithms.

We then test our algorithms in the following settings:

Case 1: We pick $m = n = 5000$, $r = 5$, sampling ratio of around 10% and sparsity of 10%. We tune $t_U = 2/|\Omega|$, $\epsilon_0 = 30$ for both AManPGC and ManPGC.

Case 2: We pick $m = 1000$, $n = 30000$, $r = 5$. sampling ratio of around 10% and sparsity of 10%. We tune $t_U = 2/|\Omega|$, $\epsilon_0 = 30$ for both AManPGC and ManPGC.

Case 3: We pick $m = n = 10000$, $r = 5$. sampling ratio of around 10% and sparsity of 10%. We tune $t_U = 2/|\Omega|$, $\epsilon_0 = 30$ for both AManPGC and ManPGC.

Case 4: We pick $m = n = 2000$, $r = 10$, sampling ratio of around 20% and sparsity of 10%. We tune $t_U = 2/|\Omega|$, $\epsilon_0 = 30$ for AManPGC and $t_U = 1.6/|\Omega|$, $\epsilon_0 = 20$ for ManPGC.

Case 5: We pick $m = n = 5000$, $r = 10$, sampling ratio of around 10% and sparsity of 10%. We tune $t_U = 2/|\Omega|$, $\epsilon_0 = 30$ for both AManPGC and ManPGC.

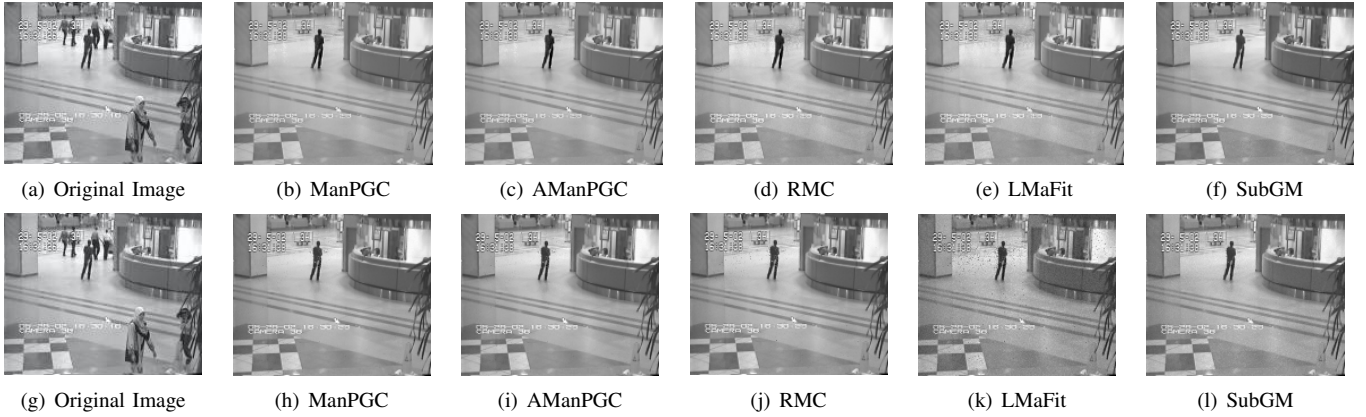


Fig. 2. Background estimation for “Hall of a business building” video data. The first row are recovered from 50% observed pixels and the second row are recovered from 10% observed pixels. (a), (g) One of the original image frame. (b), (h) Background frame estimated by ManPGC. (c), (i) Background frame estimated by AManPGC. (d), (j) Background frame estimated by RMC [5]. (e), (k) Background frame estimated by LMaFit [10]. (f), (l) Background frame estimated by SubGM [12].

TABLE I
CPU TIME AND ITERATION NUMBER COMPARISON (DATASET 1).

Algorithm	AManPGC	ManPGC	RMC	LMaFit	SubGM
CPU time (50%)	1.53	1.67	3.55	15.90	5.78
Iteration number (50%)	9	10	14	31	50
CPU time (10%)	1.02	0.91	1.56	13.44	1.07
Iteration number (10%)	11	12	30	27	60

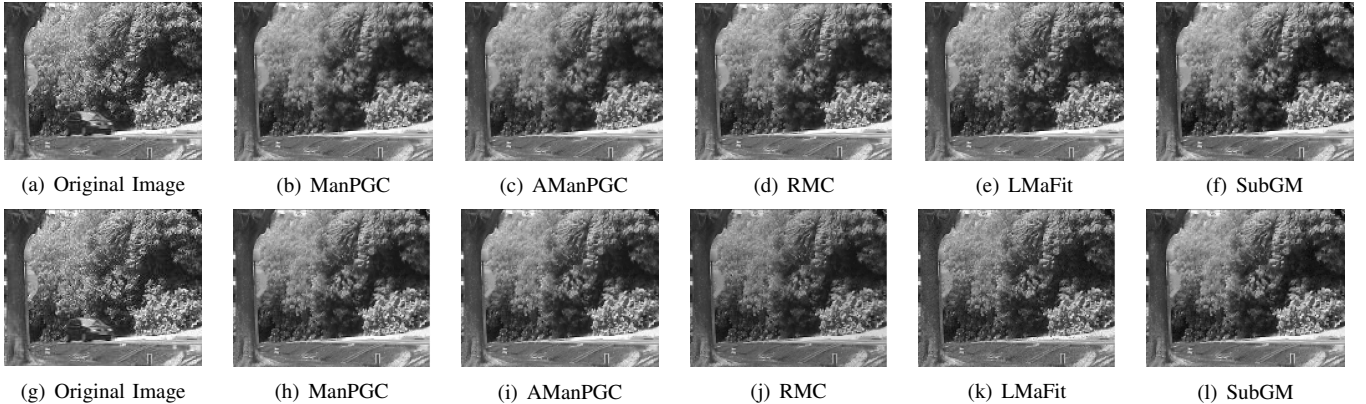


Fig. 3. Background estimation for “Campus Trees” video data. The first row are recovered from 50% observed pixels and the second row are recovered from 10% observed pixels. (a), (g) One of the original image frame. (b), (h) Background frame estimated by ManPGC. (c), (i) Background frame estimated by AManPGC. (d), (j) Background frame estimated by RMC [5]. (e), (k) Background frame estimated by LMaFit [10]. (f), (l) Background frame estimated by SubGM [12].

Case 6: We pick $m = n = 5000$, $r = 5$, sampling ratio of around 20% and sparsity of 10%. We tune $t_U = 2/|\Omega|$, $\epsilon_0 = 30$ for both AManPGC and ManPGC.

Case 7: We pick $m = n = 5000$, $r = 5$, sampling ratio of around 10% and sparsity of 20%. We tune $t_U = 2/|\Omega|$, $\epsilon_0 = 30$ for both AManPGC and ManPGC.

Case 8: We pick $m = n = 10000$, $r = 5$, sampling ratio of around 20% and sparsity of 10%. We tune $t_U = 2/|\Omega|$, $\epsilon_0 = 100$ for both AManPGC and ManPGC.

In the k -th iteration, we calculate the relative difference for each method as

$$\text{Relative Difference}(k) = \frac{\|U^k V^k - X^*\|_F}{\|X^*\|_F}, \quad (35)$$

and report the Relative Difference versus both CPU time (second) and iteration number in Figure 1.

From Figure 1, we can see that the proposed ManPGC and AManPGC algorithms outperform all other baseline algorithms on both CPU time and number of iterations for all cases. It also shows that for most cases, AManPGC performs better than ManPGC.

B. Real Data: Video Background Estimation from Partial Observation

We now evaluate the performance of ManPGC and AManPGC for video background estimation [35]. By stacking the columns of each frame into a long vector, we obtain a low-rank plus sparse matrix with the almost fixed background as the

TABLE II
CPU TIME AND ITERATION NUMBER COMPARISON (DATASET 2).

Algorithm	AManPGC	ManPGC	RMC	LMaFit	SubGM
CPU time (50%)	1.76	1.56	3.21	13.42	3.78
Iteration number (50%)	7	7	17	26	50
CPU time (10%)	0.82	0.67	2.31	10.93	1.76
Iteration number (10%)	9	11	26	28	50

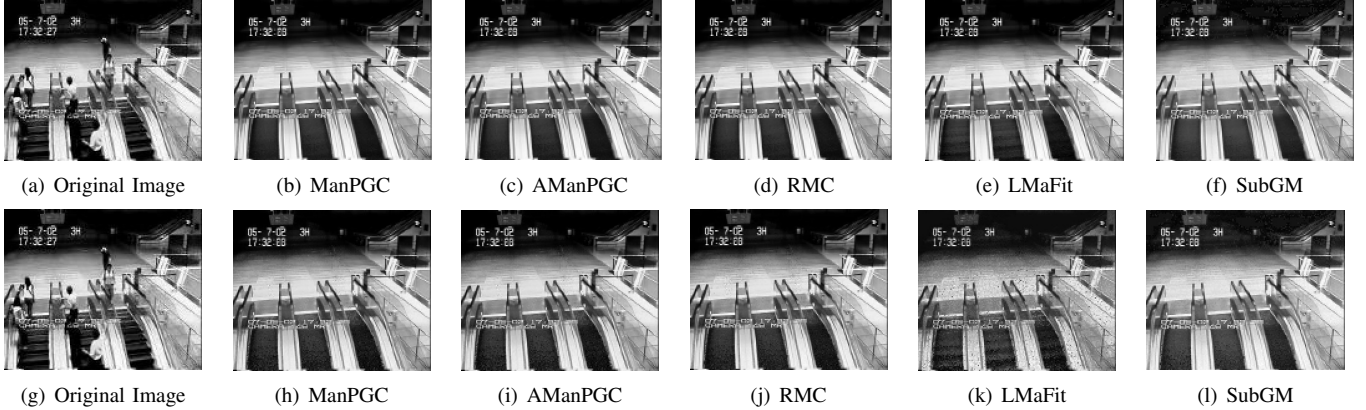


Fig. 4. Background estimation for “Airport Elevator” video data. The first row are recovered from 50% observed pixels and the second row are recovered from 10% observed pixels. (a), (g) One of the original image frame. (b), (h) Background frame estimated by ManPGC. (c), (i) Background frame estimated by AManPGC. (d), (j) Background frame estimated by RMC [5]. (e), (k) Background frame estimated by LMaFit [10]. (f), (l) Background frame estimated by SubGM [12].

TABLE III
CPU TIME AND ITERATION NUMBER COMPARISON (DATASET 3).

Algorithm	AManPGC	ManPGC	RMC	LMaFit	SubGM
CPU time (50%)	1.61	1.37	2.70	9.97	3.65
Iteration number (50%)	8	8	26	25	60
CPU time (10%)	0.74	0.95	1.72	9.12	1.08
Iteration number (10%)	15	15	28	26	60

low-rank part. In this case, we observe that even if we only have partial observation for each video frame, we still recover the whole background with very good quality. Additionally, using partial observation speeds up the background reconstruction process since we need less computation in each iteration for all algorithms. We apply all algorithms for the background estimation to three surveillance video datasets: “Hall of a business building”, “Campus Trees” and “Airport Elevator”. In our implementation, the observed pixels are randomly picked from the stacked matrix.

Dataset 1: “Hall of a business building” video is a sequence of 300 grayscale frames of size 144×176 . So the matrix $X^* \in \mathbb{R}^{25344 \times 300}$.

Dataset 2: “Campus Trees” video is a sequence of 994 grayscale frames of size 128×160 . So the matrix $X^* \in \mathbb{R}^{20480 \times 994}$.

Dataset 3: “Airport Elevator” video is a sequence of 997 grayscale frames of size 130×160 . So the matrix $X^* \in \mathbb{R}^{20800 \times 997}$.

We set $r = 2$ and test two cases when we have 50% and 10% observed pixels for each dataset. We terminate each algorithm

when the recovered matrix is stable. Specifically, we stop each algorithm when the following inequality is satisfied:

$$\frac{\|U^k V^k - U^{k-1} V^{k-1}\|_F}{\|U^{k-1} V^{k-1}\|_F} \leq \delta, \quad (36)$$

where we choose $\delta = 0.01$ for all cases. We report the background pictures, the running time and the number of iterations in Figure 2, Figure 3, Figure 4, and Table I, Table II, Table III.

From Figure 2, Figure 3, Figure 4, and Table I, Table II, Table III, we conclude that when we have 50% observed pixels, all algorithms can recover the background to a very high quality. Furthermore, the proposed ManPGC and AManPGC algorithms can recover the background using the least number of iterations and run the fastest among all algorithms. We see that 10% observed pixels also can give a good recovery and it further reduces the running time and the iteration numbers for all algorithms. In each case, our proposed ManPGC and AManPGC algorithms still run the fastest. It is reported in [36] that when we have full observation of the RPCA, recovering the background for Dataset 1 takes at least 18 seconds. Here by only using partial observations, we finish the same task in

less than one second, which shows the advantages of partial observation background recovery.

VII. CONCLUSION

In this paper, we have proposed a new formulation for RMC over Grassmann Manifold. Inspired by recent work of ManPG, we have developed a new algorithm called AManPGC for solving this nonconvex nonsmooth manifold optimization problem. We have provided rigorous analysis for the convergence of AManPG algorithm. In our numerical experiments, we have tested our proposed formulation and algorithms for both synthetic and real datasets. Both experiments show that our proposed methods outperform the state-of-the-art methods.

APPENDIX A PROOF OF LEMMA V.6

Proof. For fixed $U \in \mathcal{M}$ and $S \in \mathbb{R}^{m \times n}$, define

$$g_{U,S}(T) := \langle \nabla_S f(U, S), T \rangle + \frac{1}{2t_S} \|T\|_F^2 + h(S + T).$$

It is obvious that $g_{U,S}$ is $(1/t_S)$ -strongly convex, so we have

$$g_{U,S}(T_1) \geq g_{U,S}(T_2) + \langle \partial g_{U,S}(T_2), T_1 - T_2 \rangle + \frac{1}{2t_S} \|T_1 - T_2\|_F^2, \quad \forall T_1, T_2 \in \mathbb{R}^{m \times n}. \quad (37)$$

By letting $T_1 = 0$, $T_2 = \Delta S^k$ in (37), we have

$$\begin{aligned} g_{U^k, S^k}(0) &\geq g(\Delta S^k) - \langle \partial g_{U^k, S^k}(\Delta S^k), \Delta S^k \rangle \\ &\quad + \frac{1}{2t_S} \|\Delta S^k\|_F^2 \\ &= g_{U^k, S^k}(\Delta S^k) + \frac{1}{2t_S} \|\Delta S^k\|_F^2, \end{aligned} \quad (38)$$

where the equality is from the optimality condition of (29a), i.e., $0 \in \partial g_{U^k, S^k}(\Delta S^k)$. Using Assumption V.2, we can get

$$\begin{aligned} f(U^k, S^{k+1}) - f(U^k, S^k) &\leq \langle \nabla_S f(U^k, S^k), \Delta S^k \rangle \\ &\quad + \frac{L_S}{2} \|\Delta S^k\|_F^2. \end{aligned} \quad (39)$$

Therefore

$$\begin{aligned} &F(U^k, S^{k+1}) - F(U^k, S^k) \\ &= f(U^k, S^{k+1}) - f(U^k, S^k) + h(S^k + \Delta S^k) - h(S^k) \\ &\leq \langle \nabla_S f(U^k, S^k), \Delta S^k \rangle + \frac{L_S}{2} \|\Delta S^k\|_F^2 \\ &\quad + h(S^k + \Delta S^k) - h(S^k) \\ &= \frac{L_S}{2} \|\Delta S^k\|_F^2 + g(\Delta S^k) - \frac{1}{2t_S} \|\Delta S^k\|_F^2 - g(0) \\ &\leq \left(\frac{L_S}{2} - \frac{1}{t_S} \right) \|\Delta S^k\|_F^2 \\ &= -\frac{L_S}{2} \|\Delta S^k\|_F^2, \end{aligned}$$

where the first inequality comes from (39), and the second inequality is from (38). This completes the proof. \square

APPENDIX B PROOF OF LEMMA V.7

Proof. From Assumption V.3, we have

$$\begin{aligned} &F(U^{k+1}, S^{k+1}) - F(U^k, S^{k+1}) \\ &= f(U^{k+1}, S^{k+1}) - f(U^k, S^{k+1}) \\ &\leq f(\text{Retr}_{U^k}(\Delta U^k), S^{k+1}) - f(U^k, S^{k+1}) \\ &\leq \langle \Delta U^k, \text{grad}_{U^k} f(U^k, S^{k+1}) \rangle + \frac{L_U}{2} \|\Delta U^k\|_F^2 \\ &\leq \left(\frac{L_U}{2} - \frac{1}{t_U} \right) \|\Delta U^k\|_F^2 \\ &= -\frac{L_U}{2} \|\Delta U^k\|_F^2, \end{aligned}$$

where the second inequality is due to (31). This completes the proof. \square

APPENDIX C PROOF OF THEOREM V.8

Proof. Combining (33) and (34) yields,

$$\begin{aligned} &F(U^{k+1}, S^{k+1}) - F(U^k, S^k) \\ &= F(U^{k+1}, S^{k+1}) - F(U^k, S^{k+1}) + F(U^k, S^{k+1}) \\ &\quad - F(U^k, S^k) \\ &\leq -\frac{L_S}{2} \|\Delta S^k\|_F^2 - \frac{L_U}{2} \|\Delta U^k\|_F^2 \\ &\leq -\frac{L}{2} \left(\|\Delta S^k\|_F^2 + \|\Delta U^k\|_F^2 \right). \end{aligned} \quad (40)$$

Since F is decreasing and bounded below, we have

$$\lim_{k \rightarrow \infty} \left(\|\Delta S^k\|_F^2 + \|\Delta U^k\|_F^2 \right) = 0.$$

It follows that every limit point of $\{(U^k, S^k)\}$ is a stationary point of (28). Moreover, if AManPG (29) does not terminate after K iterations, i.e., (32) is not satisfied, we have

$$\left(\|\Delta S^k\|_F^2 + \|\Delta U^k\|_F^2 \right) > \epsilon^2/L^2, \quad \text{for } k = 0, 1, \dots, K.$$

Then summing (40) over $k = 0, \dots, K-1$, we have

$$\begin{aligned} F(U^0, S^0) - F_* &\geq F(U^0, S^0) - F(U^K, S^K) \\ &\geq \sum_{k=0}^{K-1} \frac{L}{2} \left(\|\Delta S^k\|_F^2 + \|\Delta U^k\|_F^2 \right) \\ &\geq \frac{K\epsilon^2}{2L}. \end{aligned} \quad (41)$$

Therefore, the AManPG (29) with termination criterion (32) finds an ϵ -stationary point of problem (28) in at most $\lceil 2L(F(X^0) - F_*)/\epsilon^2 \rceil$ iterations. \square

REFERENCES

- [1] Y. Koren, R. Bell, and C. Volinsky, "Matrix factorization techniques for recommender systems," *Computer*, vol. 42, no. 8, pp. 30–37, Aug 2009.
- [2] J. Wright, A. Ganesh, S. Rao, Y. Peng, and Y. Ma, "Robust principal component analysis: Exact recovery of corrupted low-rank matrices via convex optimization," in *Advances in neural information processing systems*, Vancouver, Canada, Dec 2009, pp. 2080–2088.
- [3] Y. Koren, "Factorization meets the neighborhood: a multifaceted collaborative filtering model," in *Proceedings of the 14th ACM SIGKDD international conference on Knowledge discovery and data mining*, Las Vegas, NV, Aug 2008, pp. 426–434.

- [4] R. Otazo, E. Candes, and D. K. Sodickson, "Low-rank plus sparse matrix decomposition for accelerated dynamic mri with separation of background and dynamic components," *Magnetic resonance in medicine*, vol. 73, no. 3, pp. 1125–1136, Mar 2015.
- [5] L. Cambier and P.-A. Absil, "Robust low-rank matrix completion by riemannian optimization," *SIAM Journal on Scientific Computing*, vol. 38, no. 5, pp. S440–S460, Oct 2016.
- [6] S. Ma and N. S. Aybat, "Efficient optimization algorithms for robust principal component analysis and its variants," *Proceedings of the IEEE*, vol. 106, no. 8, pp. 1411–1426, Jun 2018.
- [7] X. Guo and Z. Lin, "Low-rank matrix recovery via robust outlier estimation," *IEEE Transactions on Image Processing*, vol. 27, no. 11, pp. 5316–5327, Nov 2018.
- [8] X. Cao, Q. Zhao, D. Meng, Y. Chen, and Z. Xu, "Robust low-rank matrix factorization under general mixture noise distributions," *IEEE Transactions on Image Processing*, vol. 25, no. 10, pp. 4677–4690, Oct 2016.
- [9] Y. Chen and M. J. Wainwright, "Fast low-rank estimation by projected gradient descent: General statistical and algorithmic guarantees," *arXiv preprint arXiv:1509.03025*, 2015.
- [10] Y. Shen, Z. Wen, and Y. Zhang, "Augmented lagrangian alternating direction method for matrix separation based on low-rank factorization," *Optimization Methods and Software*, vol. 29, no. 2, pp. 239–263, Jul 2014.
- [11] L. Zhao, P. Babu, and D. P. Palomar, "Efficient algorithms on robust low-rank matrix completion against outliers," *IEEE Transactions on Signal Processing*, vol. 64, no. 18, pp. 4767–4780, May 2016.
- [12] X. Li, Z. Zhu, A. Man-Cho So, and R. Vidal, "Nonconvex robust low-rank matrix recovery," *SIAM Journal on Optimization*, vol. 30, no. 1, pp. 660–686, Feb 2020.
- [13] W. Dai, O. Milenkovic, and E. Kerman, "Subspace evolution and transfer (SET) for low-rank matrix completion," *Signal Processing, IEEE Transactions on*, vol. 59, no. 7, pp. 3120–3132, Jul 2011.
- [14] W. Dai, E. Kerman, and O. Milenkovic, "A geometric approach to low-rank matrix completion," *Information Theory, IEEE Transactions on*, vol. 58, no. 1, pp. 237–247, Jan 2012.
- [15] R. H. Keshavan, A. Montanari, and S. Oh, "Low-rank matrix completion with noisy observations: a quantitative comparison," in *Proceedings of the 47th Allerton Conference in Communication, Control, and Computing*, Allerton House, IL, Sep 2009.
- [16] R. H. Keshavan and S. Oh, "OptSpace: A gradient descent algorithm on the Grassman manifold for matrix completion," *arXiv:0910.5260*, 2009.
- [17] J. He, L. Balzano, and J. Lui, "Online robust subspace tracking from partial information," *arXiv preprint arXiv:1109.3827*, 2011.
- [18] J. He, L. Balzano, and A. Szlam, "Incremental gradient on the Grassmannian for online foreground and background separation in subsampled video," in *Proceedings of the 25th IEEE Conference on Computer Vision and Pattern Recognition (CVPR 2012)*, Providence, RI, Jun 2012.
- [19] E. T. Hale, W. Yin, and Y. Zhang, "Fixed-point continuation for ℓ_1 -minimization: Methodology and convergence," *SIAM Journal on Optimization*, vol. 19, no. 3, pp. 1107–1130, Oct 2008.
- [20] E. J. Candès, X. Li, Y. Ma, and J. Wright, "Robust principal component analysis?" *Journal of the ACM (JACM)*, vol. 58, no. 3, p. 11, Jun 2011.
- [21] V. Chandrasekaran, S. Sanghavi, P. A. Parrilo, and A. S. Willsky, "Rank-sparsity incoherence for matrix decomposition," *SIAM Journal on Optimization*, vol. 21, no. 2, pp. 572–596, Jun 2011.
- [22] N. Boumal and P.-A. Absil, "RTRMC: A Riemannian trust-region method for low-rank matrix completion," in *Proceedings of the 25th Annual Conference on Neural Information Processing Systems (NeurIPS 2011)*, Granada, Spain, Dec 2011, pp. 406–414.
- [23] —, "Low-rank matrix completion via preconditioned optimization on the Grassmann manifold," *Linear Algebra and its Applications*, vol. 475, pp. 200–239, Jun 2015.
- [24] Y. He, F. Wang, Y. Li, J. Qin, and B. Chen, "Robust matrix completion via maximum correntropy criterion and half-quadratic optimization," *IEEE Transactions on Signal Processing*, vol. 68, pp. 181–195, Nov 2019.
- [25] W.-J. Zeng and H. C. So, "Outlier-robust matrix completion via ℓ_p -minimization," *IEEE Transactions on Signal Processing*, vol. 66, no. 5, pp. 1125–1140, Mar 2017.
- [26] S. Zhang and M. Wang, "Correction of corrupted columns through fast robust hankel matrix completion," *IEEE Transactions on Signal Processing*, vol. 67, no. 10, pp. 2580–2594, Mar 2019.
- [27] S. Chen, S. Ma, A. M.-C. So, and T. Zhang, "Proximal gradient method for nonsmooth optimization over the Stiefel manifold," *SIAM J. Optimization*, vol. 30, no. 1, pp. 210–239, Jan 2020.
- [28] P.-A. Absil, R. Mahony, and R. Sepulchre, *Optimization algorithms on matrix manifolds*. Princeton University Press, 2009.
- [29] S. Chen, S. Ma, L. Xue, and H. Zou, "An alternating manifold proximal gradient method for sparse pca and sparse cca," *arXiv preprint arXiv:1903.11576*, 2019.
- [30] S. Ma, D. Goldfarb, and L. Chen, "Fixed point and bregman iterative methods for matrix rank minimization," *Mathematical Programming*, vol. 128, no. 1-2, pp. 321–353, Sep 2011.
- [31] D. Goldfarb and S. Ma, "Convergence of fixed-point continuation algorithms for matrix rank minimization," *Foundations of Computational Mathematics*, vol. 11, no. 2, pp. 183–210, Feb 2011.
- [32] L. Xiao and T. Zhang, "A proximal-gradient homotopy method for the sparse least-squares problem," *SIAM Journal on Optimization*, vol. 23, pp. 1062–1091, May 2013.
- [33] N. Boumal, P.-A. Absil, and C. Cartis, "Global rates of convergence for nonconvex optimization on manifolds," *IMA Journal of Numerical Analysis*, vol. 39, no. 1, pp. 1–33, Jan 2018.
- [34] W. H. Yang, L.-H. Zhang, and R. Song, "Optimality conditions for the nonlinear programming problems on riemannian manifolds," *Pacific Journal of Optimization*, vol. 10, no. 2, pp. 415–434, Jul 2014.
- [35] L. Li, W. Huang, I. Y.-H. Gu, and Q. Tian, "Statistical modeling of complex backgrounds for foreground object detection," *IEEE Transactions on Image Processing*, vol. 13, no. 11, pp. 1459–1472, Oct 2004.
- [36] X. Zhang, L. Wang, and Q. Gu, "A unified framework for nonconvex low-rank plus sparse matrix recovery," in *Proceedings of the 21st International Conference on Artificial Intelligence and Statistics*, Playa Blanca, Spain, Apr 2018.